



A note on the relationships between electronic structure and serotonin 5-HT_{1A} receptor binding affinity in a series of 4-butyl-arylpiperazine-3-(1H-indol-3-yl)pyrrolidine-2,5-dione derivatives

Juan S. Gómez-Jeria^{1,2*}, Andrés Robles-Navarro¹, Catalina Soza-Cornejo¹

¹Quantum Pharmacology Unit, Department of Chemistry, Faculty of Sciences, University of Chile. Las Palmeras 3425, Santiago 7800003, Chile

²Glowing Neurons Group, CP 8270745 Santiago, Chile

Corresponding author: facien03@uchile.cl

Abstract A Density Functional Theory analysis was performed to investigate the relationships between 5HT_{1A} receptor affinity and of group of 4-butyl-arylpiperazine-3-(1H-indol-3-yl)pyrrolidine-2,5-dione derivatives. The Klopman-Peradejordi-Gómez method was employed for the study. The electronic structure was calculated at the B3LYP/6-31g(d,p.) level with full geometry optimization. A statistically significant equation was found involving Hartree-Focklocal atomic reactivity indices of four atoms. We propose the possible interactions of these sites with the receptor.

Keywords Quantum pharmacology, 5-HT_{1A} receptor, serotonin, Klopman-Peradejordi-Gómez QSAR method, receptor affinity, molecular interactions, local atomic reactivity indices, Hartree-Fock

Introduction

Serotonin plays two significant roles in human: one central and the other peripheral depending on the location of the 5-HT pools of on either side of the blood-brain barrier [1]. In the central nervous system it acts as a neurotransmitter, controlling such brain functions as autonomic neural activity, stress response, body temperature, sleep, mood and appetite [1]. Serotonin plays a vital role as modulator of elements of our daily life such as mood, sleep, social behaviors, learning and appetite [2]. Although serotonin is best known for regulating higher functions, it is also crucial in maintaining whole body homeostasis [2].

The 5-HT_{1A} receptor is a subtype of serotonin receptor. 5-HT_{1A} is expressed in the brain, spleen, and neonatal kidney. It is a G protein-coupled receptor coupled to the G_i protein, and its activation in the brain mediates hyperpolarization and reduction of firing rate of the postsynaptic neuron [3]. 5-HT_{1A} receptor agonists decrease blood pressure and heart rate via a central mechanism by inducing peripheral vasodilation, and by stimulating the vagus nerve [3]. Vasodilation of the blood vessels in the skin via central 5-HT_{1A} activation increases heat dissipation from the organism out into the environment, causing a decrease in body temperature [3]. The activation of 5-HT_{1A} receptors has been demonstrated to impair certain aspects of memory (affecting declarative and non-declarative memory functions) and learning (due to interference with memory-encoding mechanisms), by inhibiting the release of glutamate and acetylcholine in various areas of the brain [3]. 5-HT_{1A} activation is known to improve cognitive functions associated with the prefrontal cortex, possibly via inducing prefrontal cortex dopamine and acetylcholine



release [3]. Other effects of 5-HT_{1A} activation that have been observed in scientific research include [3]: decreased aggression, increased sociability, decreased impulsivity, inhibition of drug-seeking behavior, facilitation of sex drive and arousal, inhibition of penile erection, diminished food intake, prolongation of REM sleep latency and reversal of opioid-induced respiratory depression [3-5]. Many molecular systems were synthesized and tested for their action on this receptor [6-20].

In our Unit we have analyzed for a longtime the structure-activity relationships of several groups of molecules interacting with the different serotonin receptors [21-37]. Here we present the results of a quantum-chemical analysis of the relationship between the electronic structure and the 5-HT_{1A} receptor binding affinity of a group of 4-butyl-arylpiperazine-3-(1*H*-indol-3-yl)pyrrolidine-2,5-dione derivatives.

Molecules, Methods, Models and Calculations

Method

After many years the following equation was developed to relate the electronic structure and biological activities [38-44]:

$$\begin{aligned} \log(K) = & a + b \log(M_D) + \sum_{o=1}^{\text{subs}} \rho_o + \sum_{i=1}^Z [e_i Q_i + f_i S_i^E + s_i S_i^N] + \\ & + \sum_{i=1}^Z \sum_{m=(\text{HOMO}-2)^*,i}^{(\text{HOMO})^*,i} [h_i(m) F_i(m^*) + j_i(m) S_i^E(m^*)] + \\ & + \sum_{i=1}^Z \sum_{m'=(\text{LUMO})^*,i}^{(\text{LUMO}+2)^*,i} [r_i(m') F_i(m'^*) + t_i(m') S_i^N(m'^*)] + \\ & + \sum_{i=1}^Z [g_i \mu_i^* + k_i \eta_i^* + o_i \omega_i^* + z_i \zeta_i^* + w_j Q_i^{*,\text{max}}] \end{aligned} \quad (1)$$

where M_D is the drug's mass, ρ_o is the orientational parameter of the o -th substituent (the summation runs over all the substituents considered in the study), Q_i is the net charge of atom i and S_i^E and S_i^N are, respectively, the total atomic electrophilic and nucleophilic superdelocalizabilities of Fukui et al. for atom i . $F_{i,m}$ is the Fukui index (electron population) of atom i in occupied (empty) MO m^* (m'^*). $S_i^E(m)^*$ is the orbital electrophilic superdelocalizability at occupied MO m^* of atom i and $S_i^N(m')^*$ is the orbital nucleophilic superdelocalizability at empty MO m'^* of atom i . μ_i^* , η_i^* , ω_i^* , ζ_i^* and $Q_i^{*,\text{max}}$ are, respectively, the local atomic electronic chemical potential, the local atomic hardness, the local atomic electrophilicity, the local atomic softness and the maximal amount of electronic charge that atom i may accept. These indices were developed within the Hartree-Fock-Roothaan formalism and are not the ones obtained in conceptual Density Functional Theory. In fact, they are conceptually better than them because they have the same units that the global equivalents. The molecular orbitals marked with an asterisk (*) correspond to the Local Molecular Orbitals (LMO) of each atom. For atom k , the LMOs are defined as the subset of the molecule's MOs having an electron population greater than 0.01e on k . In this study we have considered the three highest occupied local MOs and the three lowest empty local MO of each atom. The index Z in the summations is defined below.

Selection of molecules and biological activities

The molecules were selected from a recent study [45]. Their general formula and 5-HT_{1A} receptor binding affinity are displayed, respectively, in Fig. 1 and Table 2.



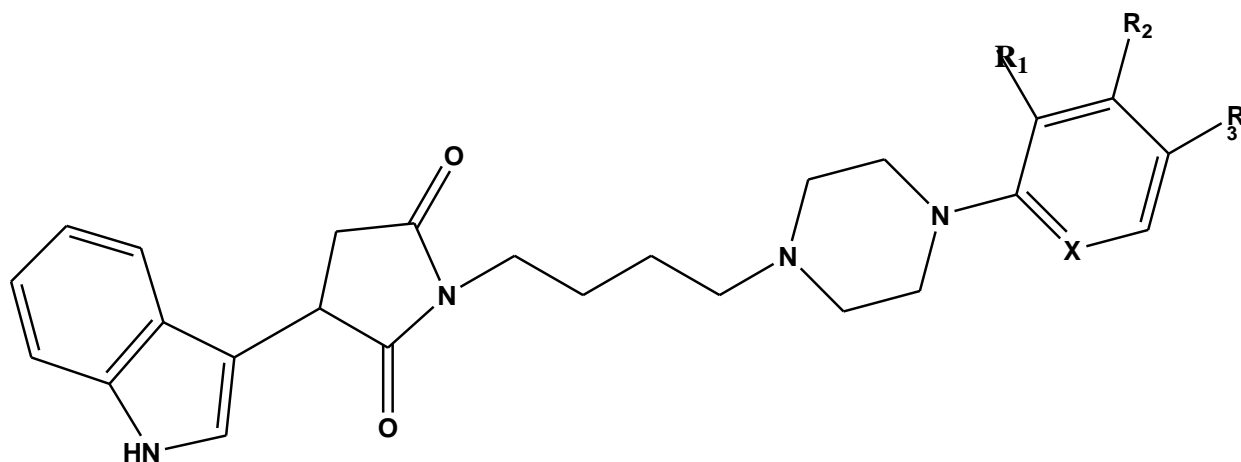


Figure 1: General formula of 4-butyl-aryl piperazine-3-(1H-indol-3-yl)pyrrolidine-2,5-dione derivatives

Table 1: 4-butyl-aryl piperazine-3-(1H-indol-3-yl)pyrrolidine-2,5-dione derivatives and 5-HT_{1A} receptor binding affinity.

	Molecule	R ₁	R ₂	R ₃	log(K)
4a	1	Cl	H	H	0.20
4b	2	H	H	Cl	1.40
4c	3	Cl	Cl	H	0.11
4d	4	F	H	H	-0.40
4e	5	H	H	F	1.62
4f	6	H	CF ₃	H	0.70
4g	7	Me	H	H	0.28
4h	8	Me	Me	H	0.18
4i	9	OMe	H	H	0.15
4j	10	H	H	OMe	1.64
4m	11	H	H	H	0.40

X=N for molecule 11.

In the next two figures we show the distribution of the data employed. Figure 2 shows the histogram of frequencies.

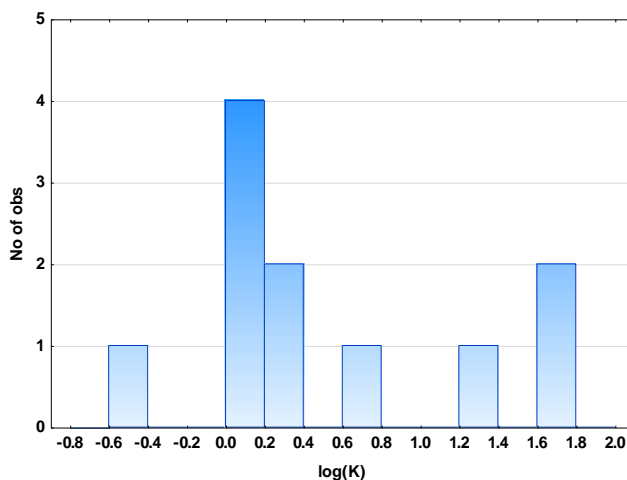


Figure 2: Histogram of frequencies



We can see that the data spans about 2 orders of magnitude and it is more or less well distributed along this interval. We cannot expect a continuous distribution of $\log(K)$ because researchers do not know what results they will get. Anyway, this molecular system was large enough to tests substitutions at other places. Figure 3 shows the Box-Whiskers plot of $\log(K)$ values with median and quartile values.

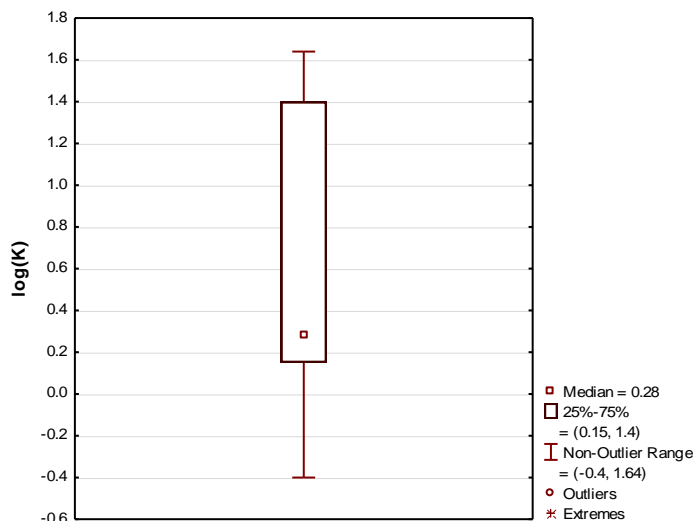


Figure 3: Box-Whiskers plot of $\log(IC_{50})$

We can see that no outliers or extremes exist.

Calculations

We employed the *common skeleton hypothesis* affirming that there is a set of atoms, common to all molecules analyzed, that accounts for a large percentage of the binding affinity. The common skeleton employed here is shown in Fig. 4 and defines the value of Z in Eq. 1 above. Atom 35 is a hydrogen atom and atoms 29-31 are the atoms directly bonded to ring E. Note that the common skeleton hypothesis is imposed by the mathematical need to have the same number of terms for each molecule in the master equation. Implicit in this hypothesis is the fact that the common skeleton of all molecules is oriented in such a way that they are all superimposed. Also, there is a great possibility that some specific atoms interacting with the site have not been included in the common skeleton because they are unique to some molecule(s) and do not have equivalents in the rest of the group.

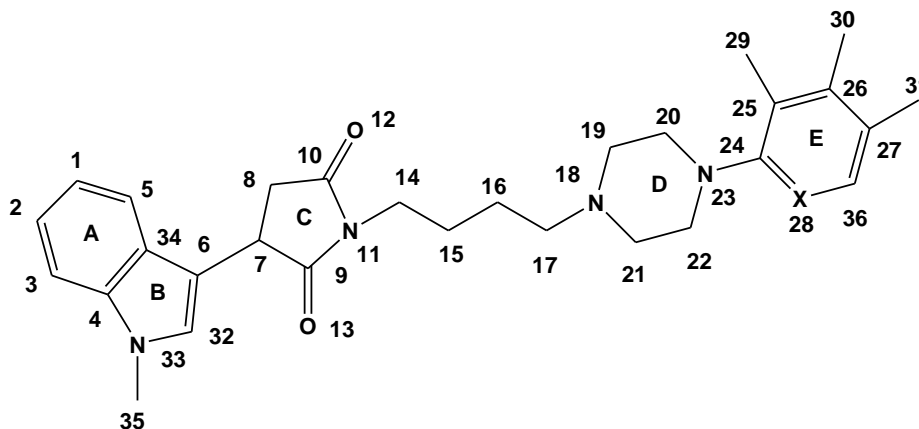


Figure 4: Common skeleton

The electronic structure of all molecules was calculated within the Density Functional Theory at the B3LYP/6-31g(d,p) level with full geometry optimization [46]. The Gaussian 16 suite of programs was used [47]. The numerical values for the local atomic reactivity indices were obtained from the Gaussian results with the D-Cent-QSAR software [48]. Negative electron populations coming from Mulliken Population Analysis were corrected [49].

As the resolution of the system of linear equations is not possible because we have not enough molecules, we made use of Linear Multiple Regression Analysis (LMRA) techniques to find the best solution. For each case, a matrix containing the dependent variable ($\log(K)$ in this case) and the local atomic reactivity indices of all atoms of the common skeleton as independent variables was built. The Statistica software was used for LMRA [50]. Let us remark that the resulting LMRA equations display at most the importance of some atoms and some substituents.

Results

The best equation obtained is:

$$\log(K) = 3.26 - 1.18F_{28}(\text{HOMO-1})^* + 3.55S_{25}^E(\text{HOMO-2})^* + 3.31S_{21}^E(\text{HOMO})^* - 0.99S_{31}^E(\text{HOMO-1})^* \quad (2)$$

with $n=11$, $R=0.99$, $R^2=0.99$, adjusted $R^2=0.98$, $F(4,6)=150.26$ ($p<0.00000$) and a standard error of estimate of 0.09. Here, $F_{28}(\text{HOMO-1})^*$ is the electron population of the second highest occupied local MO of atom 28, $S_{25}^E(\text{HOMO-2})^*$ is the electrophilic superdelocalizability of the third highest occupied local MO of atom 25, $S_{21}^E(\text{HOMO})^*$ is the electrophilic superdelocalizability of the highest occupied local MO of atom 21 and $S_{31}^E(\text{HOMO-1})^*$ is the electrophilic superdelocalizability of the second highest occupied local MO of atom 31. Tables 2 and 3 show the beta coefficients, the results of the t-test for significance of coefficients and the matrix of squared correlation coefficients for the variables of Eq. 2. There are no significant internal correlations between independent variables (Table 3). Figure 5 displays the plot of observed vs. calculated $\log(K)$.

Table 2: Beta coefficients and t-test for significance of coefficients in Eq. 2

Variable	Beta	t(6)	p-level
$F_{28}(\text{HOMO-1})^*$	-0.18	-4.15	0.006
$S_{25}^E(\text{HOMO-2})^*$	0.67	14.24	0.000007
$S_{21}^E(\text{HOMO})^*$	0.54	11.94	0.00002
$S_{31}^E(\text{HOMO-1})^*$	-0.27	-5.97	0.001

Table 3: Matrix of squared correlation coefficients for the variables in Eq. 2

	$F_{28}(\text{HOMO-1})^*$	$S_{25}^E(\text{HOMO-2})^*$	$S_{21}^E(\text{HOMO})^*$	$S_{31}^E(\text{HOMO-1})^*$
$F_{28}(\text{HOMO-1})^*$	1.00			
$S_{25}^E(\text{HOMO-2})^*$	0.02	1.00		
$S_{21}^E(\text{HOMO})^*$	0.03	0.14	1.00	
$S_{31}^E(\text{HOMO-1})^*$	0.07	0.07	0.03	1.00

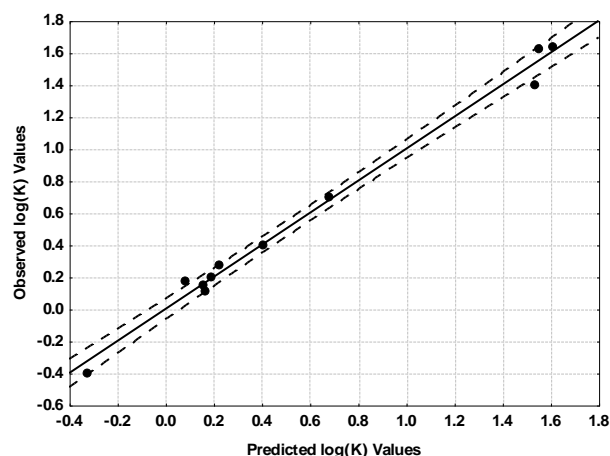


Figure 5: Plot of predicted vs. observed $\log(K)$ values (Eq. 2). Dashed lines denote the 95% confidence interval



The associated statistical parameters of Eq. 2 indicate that this equation is statistically significant and that the variation of the numerical values of a group of four local atomic reactivity indices of atoms constituting the common skeleton explains about 98% of the variation of $\log(K)$. Figure 5, spanning about 1.9 orders of magnitude, shows that there is a good correlation of observed *versus* calculated values. Figures 6, 7 and 8 show, respectively, the plot of predicted values *vs.* residuals scores, the plot of residual *vs.* deleted residuals and the normal probability plot of residuals.

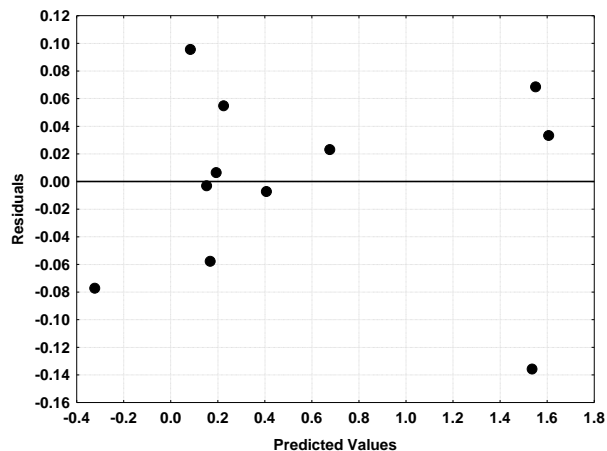


Figure 6: Plot of predicted values *vs.* residuals scores

The points do not show any kind of ordering or tendency. Therefore this plot supports the idea that the linear equation is a good first approach to study these molecules.

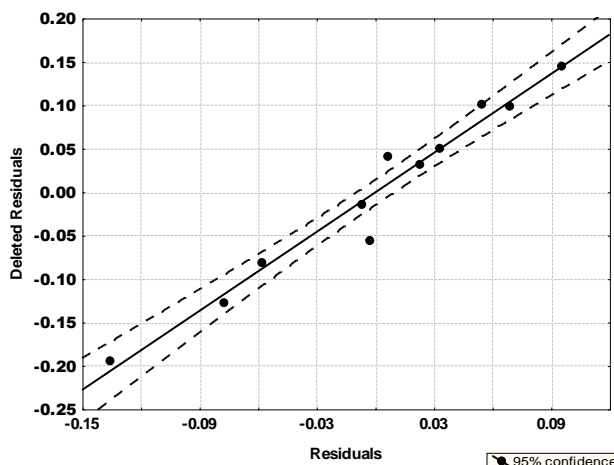


Figure 7: Plot of residual *vs.* deleted residuals

We expect that in a perfect equation all points be inside the 95% confidence interval. In this case we have two points outside the confidence interval, suggesting that these two molecules possibly have one or more interactions with the binding site through atoms that do not belong to the common skeleton. So far we have not been able to design a technique to detect these possible extra interactions.

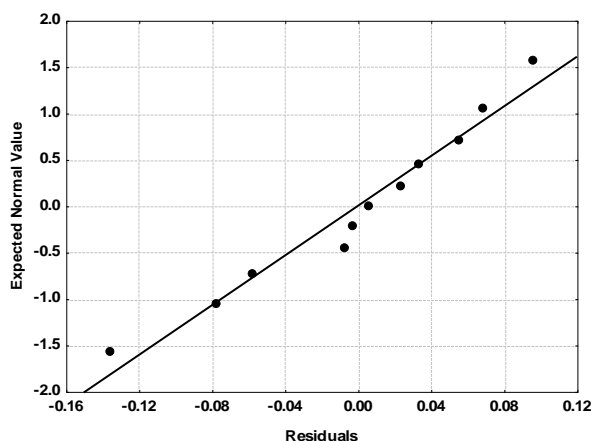


Figure 8: Normal probability plot of residuals

These three figures show that the linear equation 2 is a good first approximation to analyze the receptor binding affinity.

Local Molecular Orbitals

Table 4 shows the local MO structure of atoms 21, 25, 28 and 31 (see Fig. 4). Nomenclature: Molecule (HOMO) / (HOMO-2)* (HOMO-1)* (HOMO)* - (LUMO)* (LUMO+1)* (LUMO+2)*.

Table 4: Local Molecular Orbitals of atoms 21, 25, 28 and 31

Mol.	Atom 21	Atom 25	Atom 28	Atom 31
1 (123)	115σ121σ123σ- 127σ135σ137σ	119π121π123π- 126π127π130σ	119π121π123π- 126π127π130σ	99σ100σ113σ- 130σ135σ136σ
2 (123)	112σ121σ123σ- 135σ138σ140σ	119π121π123π- 126π127π130σ	119π121π123π- 126π127π130σ	116π121π123π- 127π130π136σ
3 (131)	123σ128σ131σ - 135σ144σ146σ	127π128π131π- 133π135π136σ	127π128π131π- 133π135π136σ	103σ105σ106σ- 136σ144σ146σ
4 (119)	111σ117σ119σ- 123σ131σ137σ	115π117π119π- 122π123π128σ	115π117π119π- 122π123π128σ	103σ104σ108σ- 128σ134σ136σ
5 (119)	109σ117σ119σ- 131σ133σ137σ	115π117π119π- 122π123π129σ	115π117π119π- 122π123π129σ	112π117π119π- 123π128σ129σ
6 (131)	123σ129σ131σ- 141σ142σ143σ	127π129π131π- 133π135π147σ	127π129π131π- 133π135π142σ	113σ116σ127σ- 133σ141σ142σ
7 (119)	109σ117σ119σ- 129σ130σ134σ	115π117π119π- 122π123π128σ	115π117π119π- 122π123π131σ	102σ103σ108σ- 129σ130σ131σ
8 (123)	117σ121σ123σ- 135σ136σ137σ	119π121π123π- 126π127π133σ	119π121π123π- 126π127π133σ	111σ112σ113σ- 132σ133σ134σ
9 (123)	113σ121σ123σ- 133σ138σ142σ	119π121π123π- 126π127π132σ	117π119π123π- 126π127π133σ	111σ112σ113σ- 132σ133σ135σ
10 (123)	118σ121σ123σ- 128σ132σ135σ	119π121π123π- 126π128π133σ	119π121π123π- 126π128π132σ	102σ111σ113σ- 132σ133σ134σ
11 (115)	104σ113σ115σ- 127σ129σ133σ	111σ113π115π- 117π119π126σ	111σ113π115π- 117π119π126σ	94σ 99σ111σ- 124σ126σ127σ

Discussion

Molecular Electrostatic Potential (MEP)

Figures 9 and 10 show, respectively, the MEP map of molecules 4 (the most active) and 10 (the less active).



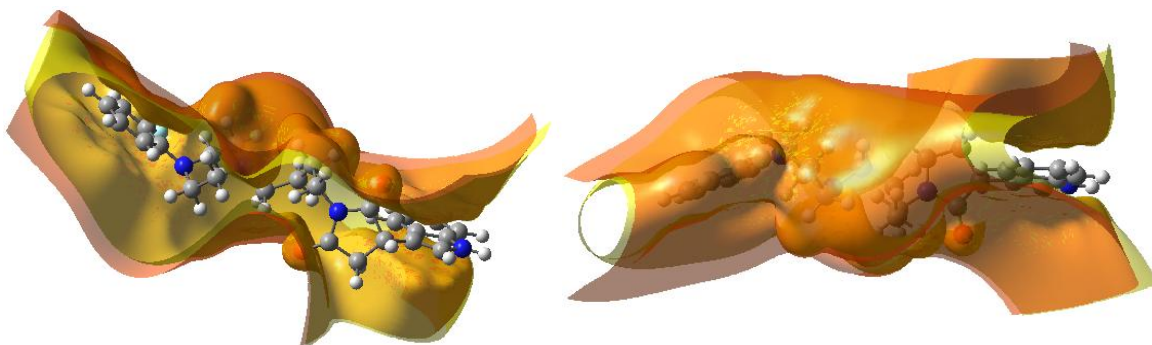


Figure 9: Two views of MEP of molecule 4 (isovalue of 0.0004, yellow is for positive and orange for negative values) [51]

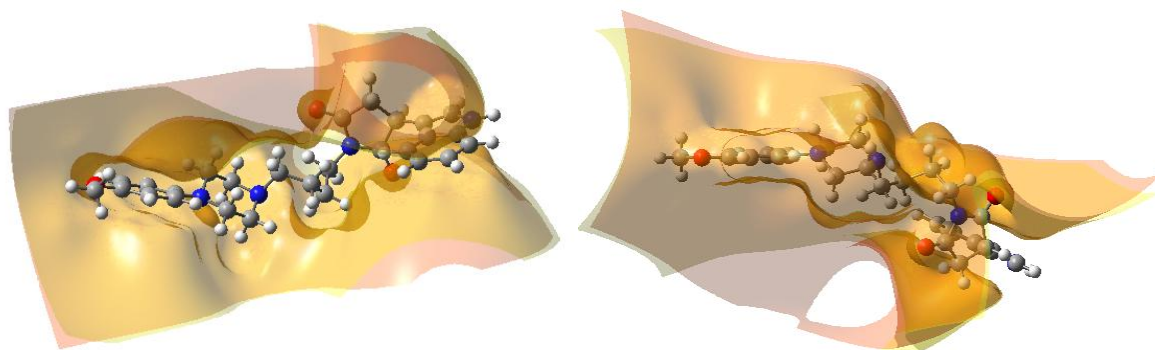


Figure 10: Two views of MEP of molecule 10 (isovalue of 0.0004, yellow color is for positive and orange for negative values)

We can see that both MEP are more or less similar despite the large difference in binding affinity. There are some differences but we cannot infer a structure-activity relationship from these MEPs. Figure 11 shows the MEP map for both molecules with a different isovalue.

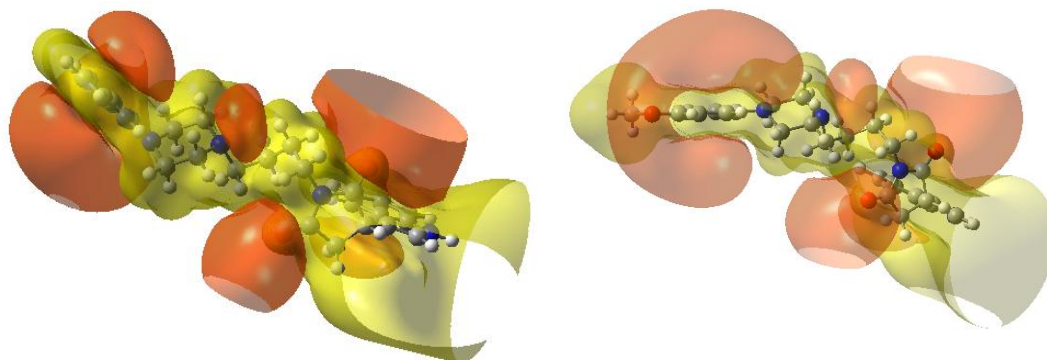


Figure 11: MEP map of molecules 4 (left) and 10 (right) for an isovalue of 0.01 [51]

These figures highlight the orange-colored sites, suitable for the approximation of an electrophile or for the interaction with an electron-deficient center or a cation. They are almost similar for both systems. The general conclusion is that MEP maps are suitable only to infer the possible structure of the MEP of the site where these molecules bind because they should be complementary. This possibility will be true if both molecules keep the same conformation when approaching the binding site.

Discussion of LMRA Result

Table 2 shows that the importance of variables in Eq. 2 is $S_{25}^E(\text{HOMO-2})^* > S_{21}^E(\text{HOMO})^* \gg S_{31}^E(\text{HOMO-1})^* > F_{28}(\text{HOMO-1})^*$. A high receptor binding affinity is associated with large numerical values for $F_{28}(\text{HOMO-1})^*$, large

(negative) numerical values for $S_{25}^E(\text{HOMO-2})^*$ and $S_{21}^E(\text{HOMO})^*$; and with small (negative) numerical values for $S_{31}^E(\text{HOMO-1})^*$. In the following analysis we have assumed that in the case of occupied MOs, every condition imposed on (HOMO-2)* affects (HOMO-1)* and (HOMO)* in the same way. Likewise, any condition imposed on (HOMO-1)* affects (HOMO)* in the same way. In the case of empty MOs, any condition imposed on (LUMO+2)* affects (LUMO+1)* and (LUMO)* in the same way. Likewise, any condition imposed on (LUMO-1)* affects (LUMO)* in the same way. Figure 12 shows the involved atoms.

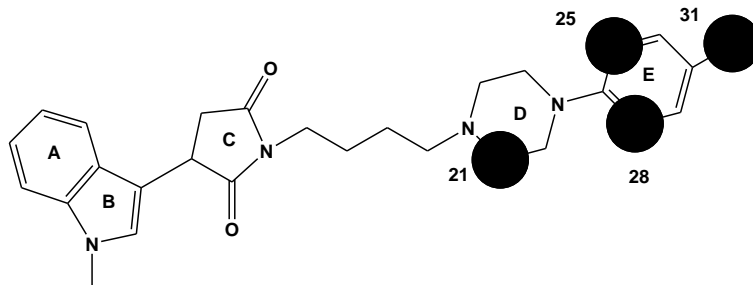


Figure 12: Atoms appearing in Eq. 2

Atom 25 is a carbon atom in ring E (Fig. 4). A high binding affinity is associated with large (negative) numerical values for $S_{25}^E(\text{HOMO-2})^*$. If we remember that [52]:

$$S_{25}^E(\text{HOMO-2})^* = F_{25}(\text{HOMO-2})^* / E_{(\text{HOMO-2})^*} \quad (3)$$

The values of $F_{25}(\text{HOMO-2})^*$ lie in the (0.01,2.0] half-open interval, severely limiting the possibilities of getting large (negative) values for $S_{25}^E(\text{HOMO-2})^*$. The other way consists in 'moving up' the energy of this OM approaching the zero of energy [53]. This will increase faster the numerical values of this reactivity index. In this case $(\text{HOMO-2})_{25}^*$ will become a better electron donor. On the other hand, $(\text{HOMO-1})_{25}^*$ and $(\text{HOMO})_{25}^*$ will also increase their reactivity. Table 4 shows that the three highest occupied local MOs of atom 25 have a pi character. This suggests that this atom is interacting with an electron-deficient center. Therefore, possible interactions can be anon-classical π -donor hydrogen bond (involving part or the entire E ring, with $d=4-4.9\text{\AA}$), $\pi-\pi$ ($d>5.5\text{\AA}$), $\pi-\sigma$ ($d=4.0-4.9\text{\AA}$), π -cation ($d=5-5.5\text{\AA}$) or π -alkyl ($d=5-5.5\text{\AA}$) kinds [54].

Atom 21 is a sp^3 carbon atom in ring D (Fig. 4). Table 4 shows that all MOs have a sigma character, that (HOMO)* coincides with the molecular HOMO and that (LUMO)* is energetically far from the molecular LUMO. Large (negative) numerical values for $S_{21}^E(\text{HOMO})^*$ are associated with high receptor binding affinity. In this case we can increase the localization of (HOMO)* on this atom to the maximum possible or move its energy towards the zero of energy as much as possible. In any case this atom seems to interact with an electron-deficient center. There are several possible types of interaction for this case. Because C-21 is a polarized atom adjacent to a nitrogen atom the first possibility is a non-classical carbon hydrogen bond C-H...X (X=O, N) ($d=3-3.9\text{\AA}$). Alkyl ($d=5-5.5\text{\AA}$) or alkyl- π ($d=5-5.5\text{\AA}$) interactions are also possible [54].

Atom 31 is the first atom of the substituent bonded to C-27 of ring D (Fig. 4). Table 1 shows that these atoms are H, F, Cl or O. A high receptor binding affinity is associated with small (negative) numerical values for $S_{31}^E(\text{HOMO-1})^*$. As this index has a similar mathematical form showed in Eq. 3, it is easy to see that these values are obtained by shifting downwards the $(\text{HOMO-1})_{31}^*$ energy. This diminishes the MO reactivity (note that the other way is by avoiding the localization of this MO on atom 31 changing it by a still lower occupied MO with lesser chemical reactivity). Using the conditions stated above, $(\text{HOMO})_{31}^*$ should also diminish its reactivity. Table 4 shows that the local HOMO* has π or σ nature (for H is always σ) and the same fact holds for local LUMO*. The only way to rationalize these different MO natures is by assuming that atom 31 is interacting with more than one site. Let us analyze these four atoms. In the case of H atoms, all Local MOs have a sigma nature (Table 4). $(\text{HOMO})_{31}^*$ and $(\text{LUMO})_{31}^*$ are energetically far from the corresponding molecular frontier MOs. In this case it seems that there could be two possibilities. The first one is the formation of a CH... X bond (with X = O, N). But atom 27 is not adjacent to an oxygen or nitrogen atom which is a requirement to form this type of bond. The distance at which this type of interaction occurs is between 3 and 3.9\AA . The other possibility is a pi-pi T-shaped interaction, in which the



hydrogen atom of the aromatic system points perpendicular to the center of another aromatic plane of another aromatic system. This interaction occurs at distances greater than 5.5Å. In this last case, the interactions of the other atoms must be compatible with the existence of an aromatic system close to that place. In the case of F and Cl Table 4 shows that the frontier local MOs have a pi nature and that local (HOMO)* coincides with the molecule's HOMO. (LUMO)₃₁* is not energetically far from the molecular LUMO. They could be involved in halogen interactions. A common moiety for both atoms is a C=O group. In the case of O, Table 4 shows that all MOs have a sigma nature and that (HOMO)₃₁* and (LUMO)₃₁* are energetically far from the corresponding molecular frontier MOs. It is possible then that this atom is involved in an O31...H-X or in an O31-H...X hydrogen bond.

Atom 28 is a C or N atom in ring E (Fig 4). A high binding affinity is associated with large numerical values for F₂₈(HOMO-1)*. Table 4 shows that (HOMO-1)₂₈*, (HOMO)₂₈* and (LUMO)₂₈* have a pi nature in all molecules. Also, (HOMO)₂₈* coincides with the molecular HOMO in all cases. Therefore, it is possible to suggest that atom 28 interacts with an electron-deficient center. Possible interactions, like in the case of C-25 (see above), can be a non-classical π -donor hydrogen bond (involving part or the entire E ring, d=4-4.9Å), π - π (d>5.5Å), π - σ (d=4.0-4.9Å), π -cation (d=5-5.5Å) or π -alkyl (d=5-5.5Å) kinds [54]. Note that atoms 25 and 28 seem to have the same kind of interactions. This allows suggesting that they could have a common interaction site. All the suggestions are displayed in the partial 2D pharmacophore of Fig. 13.

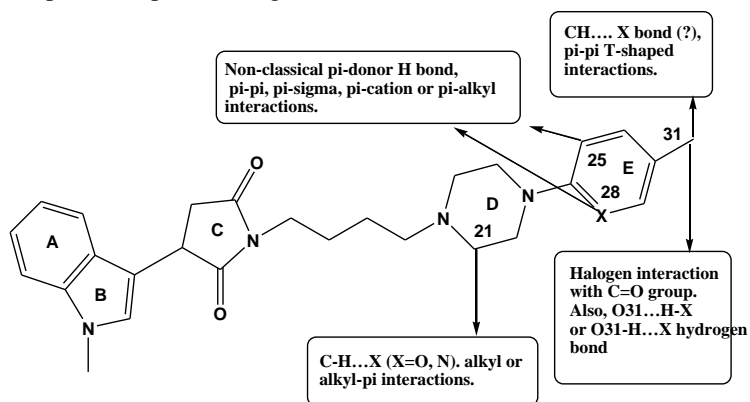


Figure 13: Partial 2D pharmacophore

In conclusion, we have obtained a statistically significant equation relating the electronic structure of a group of 4-butyl-aryl piperazine-3-(1H-indol-3-yl)pyrrolidine-2,5-dione derivatives and their 5-HT_{1A} receptor binding affinity. Four atomic centers have been identified as possible sites for possible substitutions to enhance receptor affinity.

References

- [1]. Kanova, M.; Kohout, P. Serotonin- Its Synthesis and Roles in the Healthy and the Critically Ill. *International Journal of Molecular Sciences* 2021, 22, 4837.
- [2]. Franco, R.; Rivas-Santisteban, R.; Lillo, J.; Camps, J.; Navarro, G.; Reyes-Resina, I. 5-Hydroxytryptamine, Glutamate, and ATP: Much More Than Neurotransmitters. *Frontiers in Cell and Developmental Biology* 2021, 9.
- [3]. Wikipedia. 5-HT_{1A} receptor. https://en.wikipedia.org/wiki/5-HT1A_receptor#Neuromodulation (November 14, 2021).
- [4]. Francis-Oliveira, J.; Shieh, I. C.; Vilar Higa, G. S.; Barbosa, M. A.; De Pasquale, R. Maternal separation induces changes in TREK-1 and 5HT_{1A} expression in brain areas involved in the stress response in a sex-dependent way. *Behavioural Brain Research* 2021, 396, 112909.
- [5]. Marcinkiewicz, C. A.; Bierlein-De La Rosa, G.; Dorrier, C. E.; McKnight, M.; DiBerto, J. F.; Pati, D.; Gianessi, C. A.; Hon, O. J.; Tipton, G.; McElligott, Z. A.; Delpire, E.; Kash, T. L. Sex-Dependent Modulation of Anxiety and Fear by 5-HT_{1A} Receptors in the Bed Nucleus of the Stria Terminalis. *ACS Chemical Neuroscience* 2019, 10, 3154-3166.



- [6]. Ostrowska, K.; Leśniak, A.; Czarnocka, Z.; Chmiel, J.; Bujalska-Zadrożny, M.; Trzaskowski, B. Design, Synthesis, and Biological Evaluation of a Series of 5- and 7-Hydroxycoumarin Derivatives as 5-HT_{1A} Serotonin Receptor Antagonists. *Pharmaceuticals* 2021, 14, 179.
- [7]. Ofori, E.; Onyameh, E. K.; Gonela, U. M.; Voshavar, C.; Bricker, B.; Swanson, T. L.; Eshleman, A. J.; Schmachtenberg, J. L.; Bloom, S. H.; Janowsky, A. J. New dual 5-HT_{1A} and 5-HT₇ receptor ligands derived from SYA16263. *European Journal of Medicinal Chemistry* 2021, 214, 113243.
- [8]. Zhu, C.; Li, X.; Peng, W.; Fu, W. Discovery of Novel Indolealkylpiperazine Derivatives as Potent 5-HT_{1A} Receptor Agonists for the Potential Future Treatment of Depression. *Molecules* 2020, 25, 5078.
- [9]. Sorbi, C.; Tait, A.; Battisti, U. M.; Brasili, L. Spirooxatrine derivatives towards 5-HT_{1A} receptor selectivity. *Pharmacological Reports* 2020, 72, 427-434.
- [10]. Ostrowska, K.; Leśniak, A.; Karczyńska, U.; Jeleniewicz, P.; Głuch-Lutwin, M.; Mordyl, B.; Siwek, A.; Trzaskowski, B.; Sacharczuk, M.; Bujalska-Zadrożny, M. 6-Acetyl-5-hydroxy-4,7-dimethylcoumarin derivatives: Design, synthesis, modeling studies, 5-HT_{1A}, 5-HT_{2A} and D₂ receptors affinity. *Bioorganic Chemistry* 2020, 100, 103912.
- [11]. Ma, J.; Zhang, H.; Zhang, X.; Lei, M. 3D-QSAR studies of D_{3R} antagonists and 5-HT_{1AR} agonists. *Journal of Molecular Graphics and Modelling* 2019, 86, 132-141.
- [12]. Dilly, S.; Liégeois, J.-F. Structural Insights into 5-HT_{1A}/D₄ Selectivity of WAY-100635 Analogues: Molecular Modeling, Synthesis, and in Vitro Binding. *Journal of Chemical Information and Modeling* 2016, 56, 1324-1331.
- [13]. Thio, J. P.; Liang, C.; Bajwa, A. K.; Wooten, D. W.; Christian, B. T.; Mukherjee, J. Synthesis and evaluation of mefway analogs as ligands for serotonin 5HT_{1A} receptors. *Medicinal Chemistry Research* 2015, 24, 1480-1486.
- [14]. Luo, M.; Wang, X. S.; Roth, B. L.; Golbraikh, A.; Tropsha, A. Application of Quantitative Structure–Activity Relationship Models of 5-HT_{1A} Receptor Binding to Virtual Screening Identifies Novel and Potent 5-HT_{1A} Ligands. *Journal of Chemical Information and Modeling* 2014, 54, 634-647.
- [15]. Zhu, X. Y.; Etukala, J. R.; Eyunni, S. V.; Setola, V.; Roth, B. L.; Ablordeppey, S. Y. Benzothiazoles as probes for the 5HT_{1A} receptor and the serotonin transporter (SERT): A search for new dual-acting agents as potential antidepressants. *European Journal of Medicinal Chemistry* 2012, 53, 124-132.
- [16]. Prandi, A.; Franchini, S.; Manasieva, L. I.; Fossa, P.; Cichero, E.; Marucci, G.; Buccioni, M.; Cilia, A.; Pirona, L.; Brasili, L. Synthesis, Biological Evaluation, and Docking Studies of Tetrahydrofuran-Cyclopentanone- and Cyclopentanol-Based Ligands Acting at Adrenergic α_1 - and Serotonine 5-HT_{1A} Receptors. *Journal of Medicinal Chemistry* 2012, 55, 23-36.
- [17]. Venkatesan, A. M.; Dos Santos, O.; Ellingboe, J.; Evrard, D. A.; Harrison, B. L.; Smith, D. L.; Scerni, R.; Hornby, G. A.; Schechter, L. E.; Andree, T. H. Novel benzofuran derivatives with dual 5-HT_{1A} receptor and serotonin transporter affinity. *Bioorganic & Medicinal Chemistry Letters* 2010, 20, 824-827.
- [18]. Santana, L.; Uriarte, E.; Fall, Y.; Teijeira, M.; Terán, C.; García-Martínez, E.; Tolf, B.-R. Synthesis and structure–activity relationships of new arylpiperazines: para substitution with electron-withdrawing groups decrease binding to 5-HT_{1A} and D_{2A} receptors. *European Journal of Medicinal Chemistry* 2002, 37, 503-510.
- [19]. Taverne, T.; Diouf, O.; Depreux, P.; Poupert, J. H.; Lesieur, D.; Guardiola-Lemaître, B.; Renard, P.; Rettori, M.-C.; Caignard, D.-H.; Pfeiffer, B. Novel Benzothiazolin-2-one and Benzoxazin-3-one Arylpiperazine Derivatives with Mixed 5HT_{1A}/D₂ Affinity as Potential Atypical Antipsychotics. *Journal of Medicinal Chemistry* 1998, 41, 2010-2018.
- [20]. Corsano, S.; Strappaghetta, G.; Leonardi, A.; Rhazri, K.; Barbaro, R. New 3 (2H)-pyridazinone derivatives: synthesis and affinity towards α_{1AR} subtypes and 5HT_{1A} receptors. *European Journal of Medicinal Chemistry* 1997, 32, 339-342.



- [21]. Gómez-Jeria, J. S.; Morales-Lagos, D. R. Quantum chemical approach to the relationship between molecular structure and serotonin receptor binding affinity. *Journal of Pharmaceutical Sciences* 1984, 73, 1725-1728.
- [22]. Gómez-Jeria, J. S.; Morales-Lagos, D.; Rodriguez-Gatica, J. I.; Saavedra-Aguilar, J. C. Quantum-chemical study of the relation between electronic structure and pA2 in a series of 5-substituted tryptamines. *International Journal of Quantum Chemistry* 1985, 28, 421-428.
- [23]. Gómez-Jeria, J. S.; Morales-Lagos, D.; Cassels, B. K.; Saavedra-Aguilar, J. C. Electronic structure and serotonin receptor binding affinity of 7-substituted tryptamines. *Quantitative Structure-Activity Relationships* 1986, 5, 153-157.
- [24]. Gómez-Jeria, J. S.; Cassels, B. K.; Saavedra-Aguilar, J. C. A quantum-chemical and experimental study of the hallucinogen (\pm)-1-(2,5-dimethoxy-4-nitrophenyl)-2-aminopropane (DON). *European Journal of Medicinal Chemistry* 1987, 22, 433-437.
- [25]. Gómez-Jeria, J. S.; Becerra-Ruiz, M. B. Electronic structure and rat fundus serotonin receptor binding affinity of phenethylamines and indolealkylamines. *International Journal of Advances in Pharmacy, Biology and Chemistry* 2017, 6, 72-86.
- [26]. Gómez-Jeria, J. S.; Moreno-Rojas, C. Dissecting the drug-receptor interaction with the Klopman-Peradejordi-Gómez (KPG) method. I. The interaction of 2,5-dimethoxyphenethylamines and their N-2-methoxybenzyl-substituted analogs with 5-HT_{1A} serotonin receptors. *Chemistry Research Journal* 2017, 2, 27-41.
- [27]. Gómez-Jeria, J. S.; Castro-Latorre, P.; Moreno-Rojas, C. Dissecting the drug-receptor interaction with the Klopman-Peradejordi-Gómez (KPG) method. II. The interaction of 2,5-dimethoxyphenethylamines and their N-2-methoxybenzyl-substituted analogs with 5-HT_{2A} serotonin receptors. *Chemistry Research Journal* 2018, 4, 45-62.
- [28]. Gómez-Jeria, J. S.; González-Ponce, N. A Quantum-chemical study of the relationships between electronic structure and affinities for the serotonin transporter protein and the 5-HT_{1A} receptor in a series of 2H-pyrido[1,2-c]pyrimidine derivatives. *Chemistry Research Journal* 2020, 5, 16-31.
- [29]. Gómez-Jeria, J. S.; Robles-Navarro, A. A Density Functional Theory and Docking study of the Relationships between Electronic Structure and 5-HT_{2B} Receptor Binding Affinity in N-Benzyl Phenethylamines. *Der Pharma Chemica* 2015, 7, 243-269.
- [30]. Gómez-Jeria, J. S.; Robles-Navarro, A. A Note on the Docking of some Hallucinogens to the 5-HT_{2A} Receptor. *Journal of Computational Methods in Molecular Design* 2015, 5, 45-57.
- [31]. Gómez-Jeria, J. S.; Robles-Navarro, A. DFT and Docking Studies of the Relationships between Electronic Structure and 5-HT_{2A} Receptor Binding Affinity in N-Benzylphenethylamines. *Research Journal of Pharmaceutical, Biological and Chemical Sciences* 2015, 6, 1811-1841.
- [32]. Gómez-Jeria, J. S.; Robles-Navarro, A. A Quantum Chemical Study of the Relationships between Electronic Structure and cloned rat 5-HT_{2C} Receptor Binding Affinity in N-Benzylphenethylamines. *Research Journal of Pharmaceutical, Biological and Chemical Sciences* 2015, 6, 1358-1373.
- [33]. Rickli, A.; Luethi, D.; Reinisch, J.; Buchy, D.; Hoener, M. C.; Liechti, M. E. Receptor interaction profiles of novel N-2-methoxybenzyl (NBOMe) derivatives of 2,5-dimethoxy-substituted phenethylamines (2C drugs). *Neuropharmacology* 2015, 99, 546-553.
- [34]. Gómez-Jeria, J. S.; Abuter-Márquez, J. A Theoretical Study of the Relationships between Electronic Structure and 5-HT_{1A} and 5-HT_{2A} Receptor Binding Affinity of a group of ligands containing an isonicotinic nucleus. *Chemistry Research Journal* 2017, 2, 198-213.
- [35]. Gómez-Jeria, J. S.; Moreno-Rojas, C.; Castro-Latorre, P. A note on the binding of N-2-methoxybenzyl-phenethylamines (NBOMe drugs) to the 5-HT_{2C} receptors. *Chemistry Research Journal* 2018, 3, 169-175.
- [36]. Gómez-Jeria, J. S.; Gatica-Díaz, N. A preliminary quantum chemical analysis of the relationships between electronic structure and 5-HT_{1A} and 5-HT_{2A} receptor affinity in a series of 8-acetyl-7-hydroxy-4-methylcoumarin derivatives. *Chemistry Research Journal* 2019, 4, 85-100.



- [37]. Gómez-Jeria, J. S.; Rojas-Candia, V. A DFT Investigation of the Relationships between Electronic Structure and D₂, 5-HT_{1A}, 5-HT_{2A}, 5-HT₆ and 5-HT₇ Receptor Affinities in a group of Fananserin derivatives. *Chemistry Research Journal* 2020, 5, 37-58.
- [38]. All papers of J.S.G.-J. can be found in https://www.researchgate.net/profile/Juan-Sebastian_Gomez-Jeria.
- [39]. Gómez-Jeria, J. S. On some problems in quantum pharmacology I. The partition functions. *International Journal of Quantum Chemistry* 1983, 23, 1969-1972.
- [40]. Gómez-Jeria, J. S. Modeling the Drug-Receptor Interaction in Quantum Pharmacology. In *Molecules in Physics, Chemistry, and Biology*, Maruani, J., Ed. Springer Netherlands: 1989; Vol. 4, pp 215-231.
- [41]. Gómez-Jeria, J. S.; Ojeda-Vergara, M. Parametrization of the orientational effects in the drug-receptor interaction. *Journal of the Chilean Chemical Society* 2003, 48, 119-124.
- [42]. Gómez-Jeria, J. S. A New Set of Local Reactivity Indices within the Hartree-Fock-Roothaan and Density Functional Theory Frameworks. *Canadian Chemical Transactions* 2013, 1, 25-55.
- [43]. Gómez-Jeria, J. S.; Flores-Catalán, M. Quantum-chemical modeling of the relationships between molecular structure and in vitro multi-step, multimechanistic drug effects. HIV-1 replication inhibition and inhibition of cell proliferation as examples. *Canadian Chemical Transactions* 2013, 1, 215-237.
- [44]. Paz de la Vega, A.; Alarcón, D. A.; Gómez-Jeria, J. S. Quantum Chemical Study of the Relationships between Electronic Structure and Pharmacokinetic Profile, Inhibitory Strength toward Hepatitis C virus NS5B Polymerase and HCV replicons of indole-based compounds. *Journal of the Chilean Chemical Society* 2013, 58, 1842-1851.
- [45]. Wróbel, M. Z.; Chodkowski, A.; Marciniak, M.; Dawidowski, M.; Maksymiuk, A.; Siwek, A.; Nowak, G.; Turło, J. Synthesis of new 4-butyl-arylpiperazine-3-(1H-indol-3-yl) pyrrolidine-2, 5-dione derivatives and evaluation for their 5-HT_{1A} and D₂ receptor affinity and serotonin transporter inhibition. *Bioorganic Chemistry* 2020, 97, 103662.
- [46]. The results presented here are obtained from what is now a routinary procedure. For this reason, all papers have a similar general structure. This model contains *standard* phrases for the presentation of the methods, calculations and results because they do not need to be rewritten repeatedly and because the number of possible variations to use is finite. See: Hall, S., Moskovitz, C., and Pemberton, M. 2021. Understanding Text Recycling: A Guide for Researchers. Text Recycling Research Project. Online at textrecycling.org. In.
- [47]. Frisch, M. J.; Trucks, G. W.; Schlegel, H. B.; Scuseria, G. E.; Robb, M. A.; Cheeseman, J. R.; Scalmani, G.; Barone, V.; Petersson, G. A.; Nakatsuji, H.; Li, X.; Caricato, M.; Marenich, A. V.; Bloino, J.; Janesko, B. G.; Gomperts, R.; Mennucci, B.; Hratchian, H. P. *Gaussian 16 16Rev. A.03*, Gaussian: Pittsburgh, PA, USA, 2016.
- [48]. Gómez-Jeria, J. S. *D-Cent-QSAR: A program to generate Local Atomic Reactivity Indices from Gaussian16 log files*, v. 1.0; Santiago, Chile, 2020.
- [49]. Gómez-Jeria, J. S. An empirical way to correct some drawbacks of Mulliken Population Analysis (Erratum in: *J. Chil. Chem. Soc.*, 55, 4, IX, 2010). *Journal of the Chilean Chemical Society* 2009, 54, 482-485.
- [50]. Statsoft. *Statistica v. 8.0*, 2300 East 14 th St. Tulsa, OK 74104, USA, 1984-2007.
- [51]. Dennington, R. D.; Keith, T. A.; Millam, J. M. *GaussView 5.0.8*, GaussView 5.0.8, 340 Quinpiac St., Bldg. 40, Wallingford, CT 06492, USA, 2000-2008.
- [52]. Gómez-Jeria, J. S. *Elements of Molecular Electronic Pharmacology (in Spanish)*. 1st ed.; Ediciones Sokar: Santiago de Chile, 2013; p 104.
- [53]. Gómez-Jeria, J. S.; Kpotin, G. Some Remarks on The Interpretation of The Local Atomic Reactivity Indices Within the Klopman-Peradejordi-Gómez (KPG) Method. I. Theoretical Analysis. *Research Journal of Pharmaceutical, Biological and Chemical Sciences* 2018, 9, 550-561.
- [54]. Gómez-Jeria, J. S.; Robles-Navarro, A.; Kpotin, G.; Garrido-Sáez, N.; Gatica-Díaz, N. Some remarks about the relationships between the common skeleton concept within the Klopman-Peradejordi-Gómez QSAR method and the weak molecule-site interactions. *Chemistry Research Journal* 2020, 5, 32-52.

